Experimental validation of an undersea free space laser network simulator in turbid coastal conditions

David Rashkin[a], Fraser Dalgleish[b], Ionut Cardei[a], Bing Ouyang[b], Anni Vuorenkoski[b], Mihaela Cardei[a]

[a]Florida Atlantic University, Department of Computer and Electrical Engineering and Computer Science, Boca Raton, Florida; [b]Ocean Visibility and Optics Lab, Harbor Branch Oceanographic Institute, Fort Pierce, Florida

ABSTRACT

Mobile, high throughput mid-range data communications and robust real-time data networking in the subsea environment that can accommodate high bandwidth sensors such as optical imagers have a potentially high impact as enabling technologies for a variety of future subsea operations in the areas of distributed sensing and real-time wireless feedback and control of unmanned undersea vehicles. Although much work has been done recently in the field of undersea optical free space communications and networking, to date there has yet to be an implementation of a complete multi-node undersea wireless optical data communications network. The deployment and testing of optical wireless network equipment in the undersea environment is expensive and time-consuming, and there is a clear need for a network simulation framework that will allow researchers to evaluate the performances of different networking concepts/configurations under realistic operational and environmental constraints.

This paper describes a network simulation approach that uses an accurate time dependent Monte Carlo channel model to simulate the networking physical layer, which can be used in conjunction with higher network layer protocols to simulate larger scale network performance and to help determine hardware requirements for overall network system design in a variety of undersea channel conditions.

1. INTRODUCTION

High bit rate data links (on the order of several million bits per second) with low bit error rates are required for real-time transmission of audio, video, and imagery which can be useful in a variety of applications such as environmental monitoring, commercial subsea operations, and inspection and surveillance operations. Modern terrestrial wireless communication systems such as WIFI or cellular phone networks employ radio frequency (RF) to transmit data, and while RF works very well in air, the severe attenuation of RF in water makes it impractical to use for most underwater wireless communication needs [1]. Although acoustic waves are able to travel great distances underwater, the low carrier frequencies used in the acoustic spectrum (typically between 10Hz and 1MHz) combined with the relatively slow propagation speeds of acoustic waves underwater result in low bandwidth, high latency, and low data rates [2]. Recent advances in semiconductor laser technologies have made underwater optical wireless communication a feasible alternative to acoustic and RF carriers of data. In this paper, we present a physical layer simulator for free space undersea optical wireless data links. We continue the work presented in [3], using radiometrically calibrated optical equipment (described in section 3) to validate the simulation framework (described in section 2).

Our ultimate goal is to interface the physical layer simulator with a higher level network simulator (such as OpNet or ns-2) in order to help design optimal routing protocols, multiple access, modulation and error correction schemes, and per-node power management for delay-tolerant networks (DTN) and mobile ad-hoc networks. The purpose of the experiments described in this paper is to validate the accuracy of our physical layer simulator in predicting bit error rates (BER) for a variety of pulse repetition rates and water turbidities. Our main performance metric is the 95% confidence level bit error rate (95% CL BER), which differs from a raw bit error rate in that a raw bit error rate is only useful in describing the BER for a particular data set, while a 95% CL BER can be said to predict the BER ceiling (with 95% accuracy) for all possible data sets utilizing the same environmental parameters. Maximum acceptable BER ceilings vary depending on the application, with real-time voice data requiring 10^{-2}, while TCP file downloading requires a BER ceiling on the order of 10^{-6}. Modern cellular telephone data networks such as LTE employ additional protocols that allow data transmissions with a BER ceiling of 10^{-4}.[4]

Ocean Sensing and Monitoring V, edited by Weilin W. Hou, Robert A. Arnone, Proc. of SPIE Vol. 8724, 872404 · © 2013 SPIE · CCC code: 0277-786X/13/$18 · doi: 10.1117/12.2019192

1.1 Paper Organization

In section 2, we describe our physical layer simulation framework. In section 3, we describe our experimental setup used to validate the simulation framework. Section 4 shows results from both experiments and simulations, and section 5 details conclusions, discussion, and future work.

2. NETWORK SIMULATOR

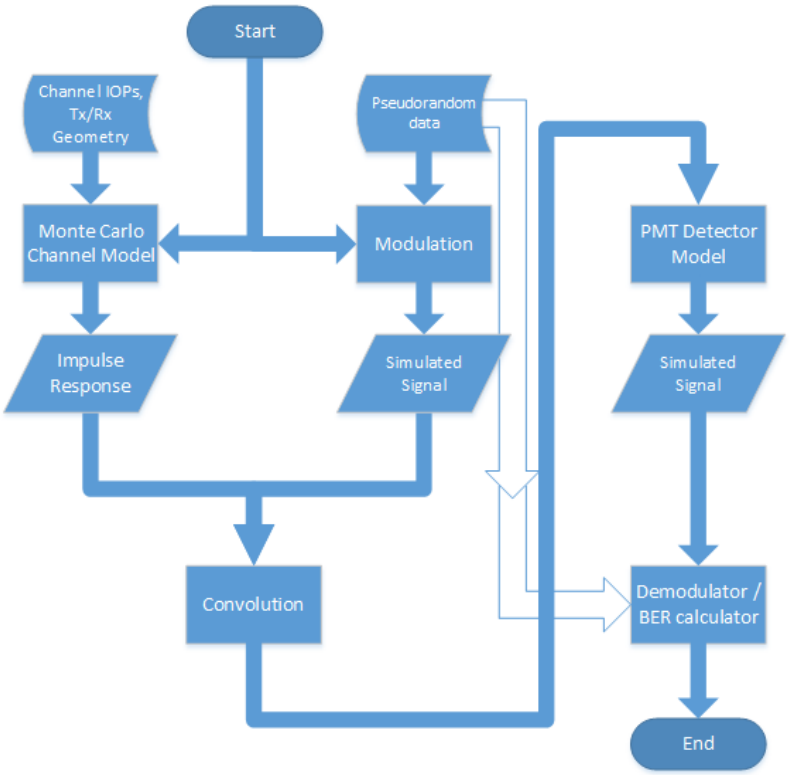

Figure 1: Physical layer simulator

Our physical layer simulator (as shown in the flowchart in Figure 1), is written in Matlab and consists of 4 main execution blocks: The modulator, the channel model, the detector model, and the demodulator.

2.1 Modulator

In this set of experiments, we used 16-slot pulse-position-modulation (PPM-16) as our modulation scheme. This allowed us to more easily isolate and analyze individual pulses, in order to compare against the experimental data. For future system design, we can easily replace the modem blocks (with OOK, for example, to maximize throughput in low-noise scenarios). The PPM-16 modulator block takes as input a bitstream (in our experiments we used a predefined pseudorandom bitstream), peak laser power, laser power variance, sampling interval and pulse repetition rate. The output is a 1-dimensional array representing the simulated signal in terms of optical power.

2.2 Channel Model

The channel model, developed by Metron, Inc., is a one-way variation of the model described in [5], and used by Vuorenkoski et. al. in [6] to demonstrate the depolarization effect of multi-path scattering on optical signals traveling through the undersea channel. This block takes as input the beam attenuation coefficient (c), the absorption coefficient (a), the scattering phase function, the position and orientation of the source and receiver in 3D space, the beam divergence, the receiver half-angle, radius, and acceptance shape. The model then simulates photon bundles traveling from the source through the medium, and outputs an impulse response based on the number of simulated photon bundles that reached the receiver.

The initial unit energy is evenly distributed among many photon bundles, each of which then travels a predetermined distance (calculated from the position and orientation parameters of the transmitter and receivers). Each photon bundle travels an average distance of 1/b (where b is the scattering coefficient) before encountering a scattering event, after which the direction of the photon bundle is changed randomly so that, on average, the distribution of scattering angles conforms to the distribution described by scattering phase function parameter. This is repeated for each photon bundle until passing through the 2D plane represented by the receiver, and the total energy passing into the receiver is obtained by summing the individual energy contributions of photons that hit the detector window. Below we describe the two-way model, which was developed for multistatic imaging applications. This two-way model can also be used to simulate non-line-of-sight (NLOS) communication links. Please note, for the experiments described in this paper, we used a one-way variation of this model, where there is no reflective object between the transmitter and receiver.

$$E_{rcv}^{scat} = \frac{R_{panel} A_{rcv}}{2\pi} \cdot \frac{E_{bundle}}{2\pi R^2} \int_0^{2\pi} W(\theta, \phi) d\phi \quad (1)$$

Equation (1) describes the two-way model where E_{rcv}^{scat} is the scattered energy at the receiver, R_{panel} is the panel reflectivity (note that in our one-way model scenario, there is no panel; the photons instead are simulated traveling directly from the source to the receiver), A_{rcv} is the receiver acceptance area, E_{bundle} is the energy contained in a photon bundle, R is the distance between transmitter and receiver, and W is the acceptance function of the receiver (for more details please see [5]).

The channel model solves the time-dependent radiative transfer equation by performing Monte Carlo simulations to create a time-dependent impulse response for the channel. It is flexible in that it allows us to specify position and orientation of a receiver in relation to a transmitter, and it also allows us to specify the position and orientation of a second receiver (placed behind [relative to the position and orientation of] the transmitter, which allows us to model the backscatter impulse response. This is important in determining under what circumstances (if any) it would be possible to use full-duplex and/or half-duplex communications at the same wavelength. By combining the two impulse responses we can also model scenarios in which non line of sight (NLOS) communications would be possible.

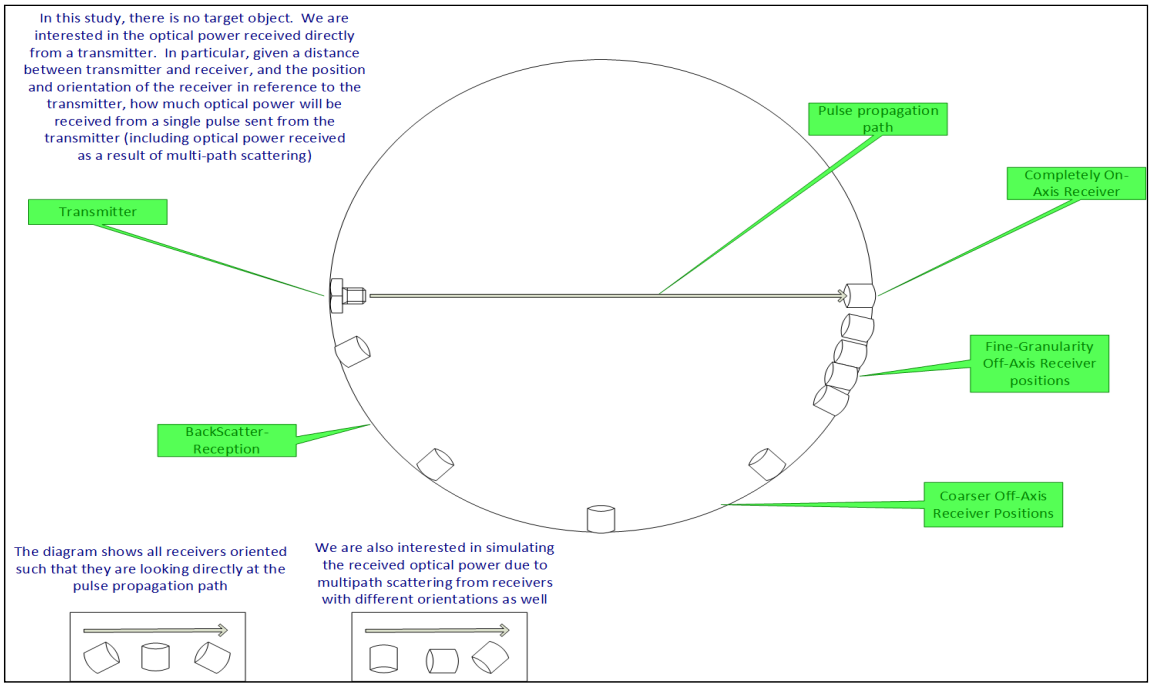

Illustration 1: Design diagram for the one-way Monte Carlo channel model code

Jaruwatanadilok described a similar model in [7], although there was no experimental validation of the results, the model assumes an ideal laser source (perfect square wave), and only considers average (mean) noise components, which may not allow for accurate BER predictions.

2.3 Photomultiplier Tube (PMT) Detector Model

This block takes as input a simulated signal, the source laser wavelength, the quantum efficiency of the detector, and the current gain applied to the PMT photocathode. The output is a signal with simulated PMT noise. PMT detectors being so-called shot noise limited devices, we ignore thermal and dark current noise and focus on predicting the shot noise introduced on the signal by the PMT. We approximate this shot noise by modeling the photomultiplier output $X(t)$ as a non-stationary compound Poisson process,

$$X(t) = \sum_{k=1}^{N(t)} G_k \, h(t - S_k) \tag{2}$$

where $N(t)$ is the number of photons striking the photocathode up to time t, S_k is the arrival time of the k^{th} photon, G_k is the random amplifier gain, and h is the electrical impulse response of the detector. A more in-depth derivation and analysis of the accuracy of this detector model in predicting per-sample noise on a simulated signal is documented in [8]. Our experimental setup used narrow bandpass filters to eliminate external noise sources such as the ambient light from our experimental data (see section 3), and instead focus on system noise introduced on the signal by the laser source (section 2.1) and the detector (section 2.3).

2.4 Demodulator

The demodulator block takes the noisy simulated signal as input, demodulates and compares against the predefined pseudorandom bitstream, and calculates the 95% CL BER. In this iteration of the simulation framework, the demodulator and the BER calculator are included in the same block, to allow us to more efficiently record pulses for later analysis and comparison against experimental data. In future iterations of the framework, the BER calculator will be separate from the demodulator block.

3. EXPERIMENTAL SETUP

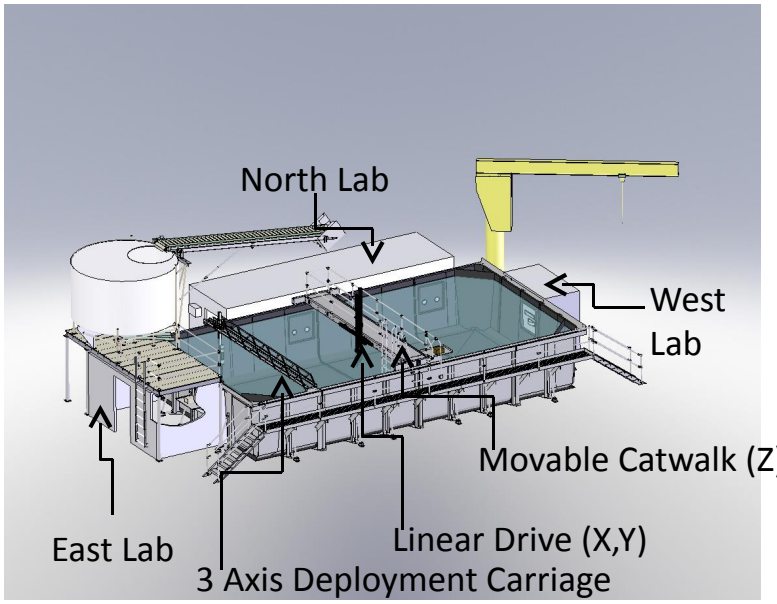

Figure 2: 12.5x7.5x2.5 m tank used for experimental data acquisition

In this set of experiments, we used a 12.5x7.5x2.5 meter saltwater tank located at the Harbor Branch Oceanographic Institute in Fort Pierce, Florida (see Figure 2). The turbidity of the water was controlled using ISO 12103-1 A1 Ultrafine Arizona Test Dust. The beam attenuation and absorption coefficients were measured using a Wet Labs AC-9 in-situ spectrophotometer. We placed a 405nm Omicron A350 laser source in the west lab, and a Hamamatsu R9880U-210 Photomultiplier Tube (PMT) detector in the east lab (12.5m apart). The laser was placed so that the beam was perpendicular to the viewport, and directed through the viewport by use of Thorlabs mirrors (see Image 1). The PMT was fitted with a 405nm narrow (3nm at full width half maximum) bandpass filter and a focusing lens that expanded the effective radius of the PMT to 5 centimeters and a 20 degree field of view. The mean output power of the laser was measured using a Nova Ophir II power meter, and found to be 10.4 mW at 6.3% duty cycle.

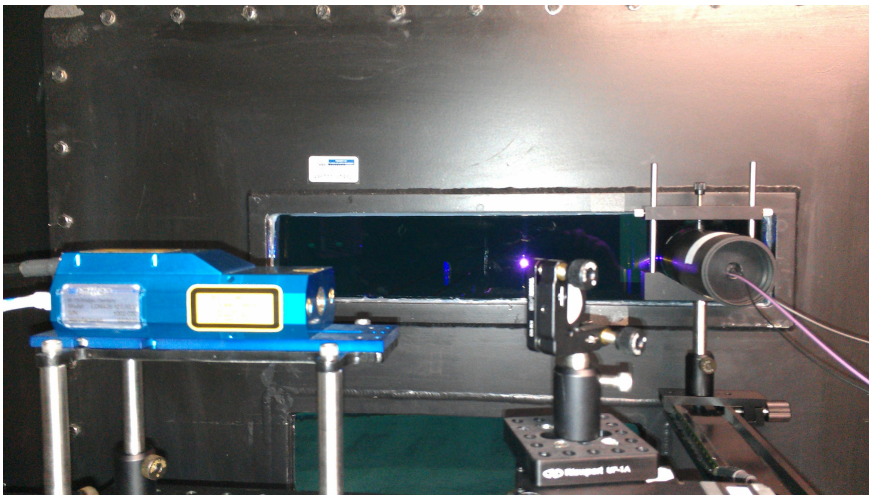

Image 1: Experimental setup, west lab. Note that the PMT pictured here is the same model (Hamamatsu R9880U-210) as the PMT in the east lab used to collect the data used in these experiments.

The lasers were driven using an Agilent 81130A high-speed pulse generator. A predefined bitstring of length 65488 (the internal memory limit of the Agilent) representing a PPM-16 modulated pseudorandom bitstream (along with a trailer for synchronization) was loaded into the internal memory and signaling was set to non-return-to-zero (NRZ). The detector outputs were attached to a National Instruments PXI 5154 high-speed 8-bit digitizer (though the dynamic range was effectively 7 bits since we were unable to set the digitizer offset to take advantage of the entire 8-bit range), set to record at 1 Gsps with a vertical range of ±0.01 V.

Using the Arizona test dust, we ran several turbidity cycles. During each cycle, we set the Agilent pulse frequency to 100MHz, 200MHz, 250MHz, and recorded 100 million samples. The gain voltage applied to the PMT was varied so that the mean voltage output of the detector remained close to 5mV (using 50Ω terminations, this corresponds to 100μA mean current through the detector, the limit for these particular PMTs).

4. RESULTS

We ran the simulator as described in section 2 using the parameters measured in our experiments described in section 3. For each turbidity cycle, we simulated transmission of 10 million samples at the data rates described in section 3 (we used 10 million samples instead of 100 million due to the computational complexity of the simulation). Comparing the simulated results to the experimental results (see figure 3 and table 1), we see very good correlations across all turbidities for the 100MHz (25Mbps effective data rate), 200 MHz (50Mbps effective data rate), and 250MHz (62.5Mbps effective data rate) cases. Note that in the 100MHz, c=0.95 case, both the simulated and experimental results contained 0 bit errors. The difference in 95% CL BER ceiling is due to the fact that we simulated 10 million samples rather than the 100 million used in the experiments.

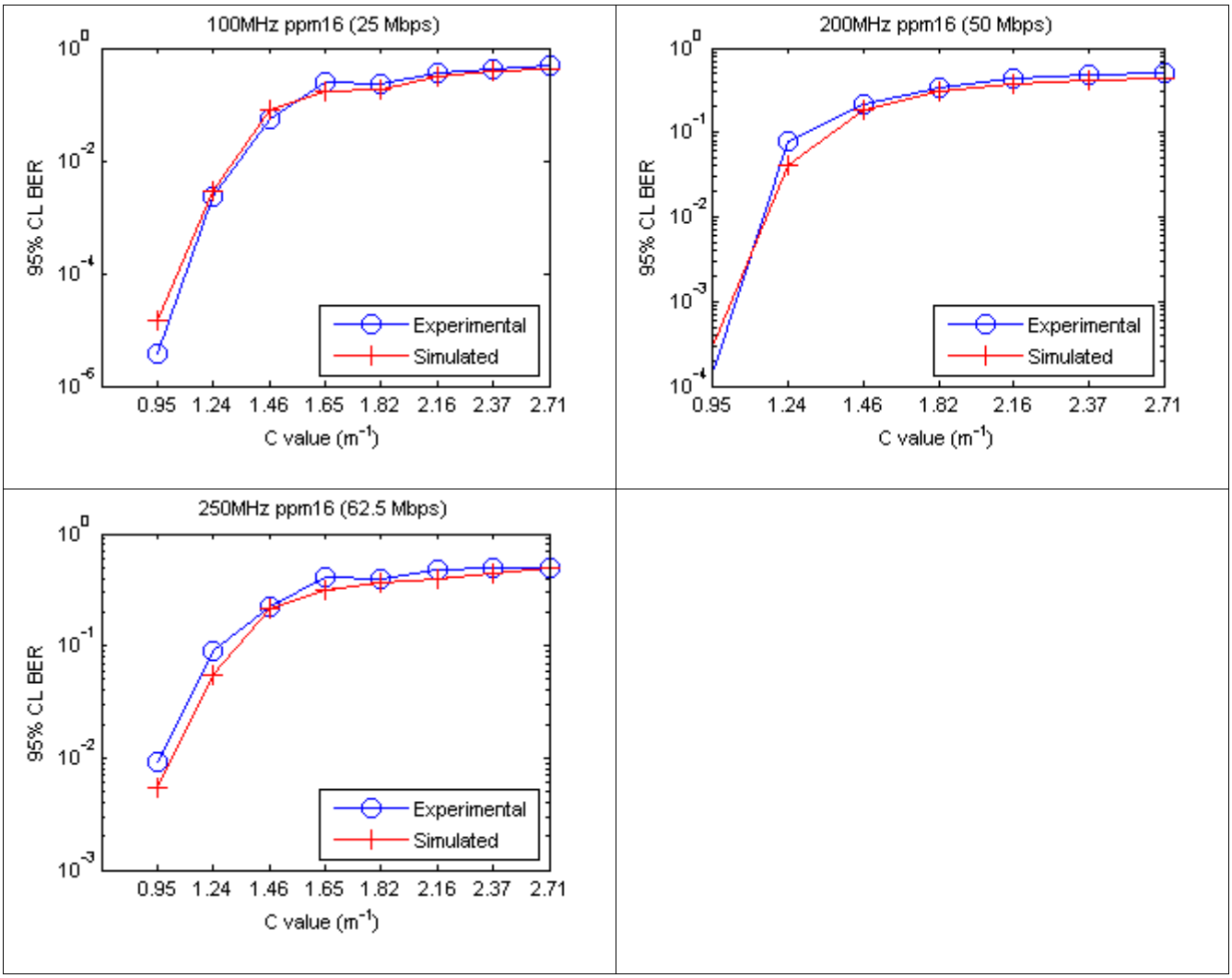

Figure 3 Experimental and simulated results for various turbidities and pulse repetition rates

Pulse repetition rate	C = 0.95	C = 1.24	C = 1.46	C = 1.65	C = 1.82	C = 2.16	C = 2.37	C = 2.71
100 MHz	Exp: 1.5e-6 Sim: 1.5e-5	Exp: 2.3e-3 Sim: 2.9e-3	Exp: 5.3e-2 Sim: 7.9e-2	Exp: 2.4e-1 Sim: 1.7e-1	Exp: 2.4e-1 Sim: 1.8e-1	Exp: 3.7e-1 Sim: 3.2e-1	Exp: 4.3e-1 Sim: 3.8e-1	Exp: 4.9e-1 Sim: 4.2e-1
200 MHz	Exp: 1.5e-4 Sim: 3.1e-4	Exp: 7.9e-2 Sim: 4.1e-2	Exp: 2.1e-1 Sim: 1.9e-1	Exp: - Sim: -	Exp: 3.4e-1 Sim: 3.0e-1	Exp: 4.5e-1 Sim: 3.7e-1	Exp: 4.8e-1 Sim: 4.2e-1	Exp: 5.0e-1 Sim: 4.3e-1
250 MHz	Exp: 9.3e-3 Sim: 5.4e-3	Exp: 8.9e-2 Sim: 5.5e-2	Exp: 2.2e-1 Sim: 2.2e-1	Exp: 4.1e-1 Sim: 3.1e-1	Exp: 3.9e-1 Sim: 3.7e-1	Exp: 4.7e-1 Sim: 3.9e-1	Exp: 5.0e-1 Sim: 4.4e-1	Exp: 5.0e-1 Sim: 5.0e-1
PMT Gain	500.75 V	622.5 V	707.75 V	707.75 V	807.75 V	915 V	987.5 V	987.5 V

Table 1: Data used to generate the charts in Figure 3

During demodulation, we recorded sample windows corresponding to pulses which were correctly demodulated. These were then averaged to arrive at the mean pulses shown in figures 4(a) – 4(f). In comparing these mean pulses, we see good alignment between experimental and simulated pulses, with full width half maximum (FWHM) values matching up well.

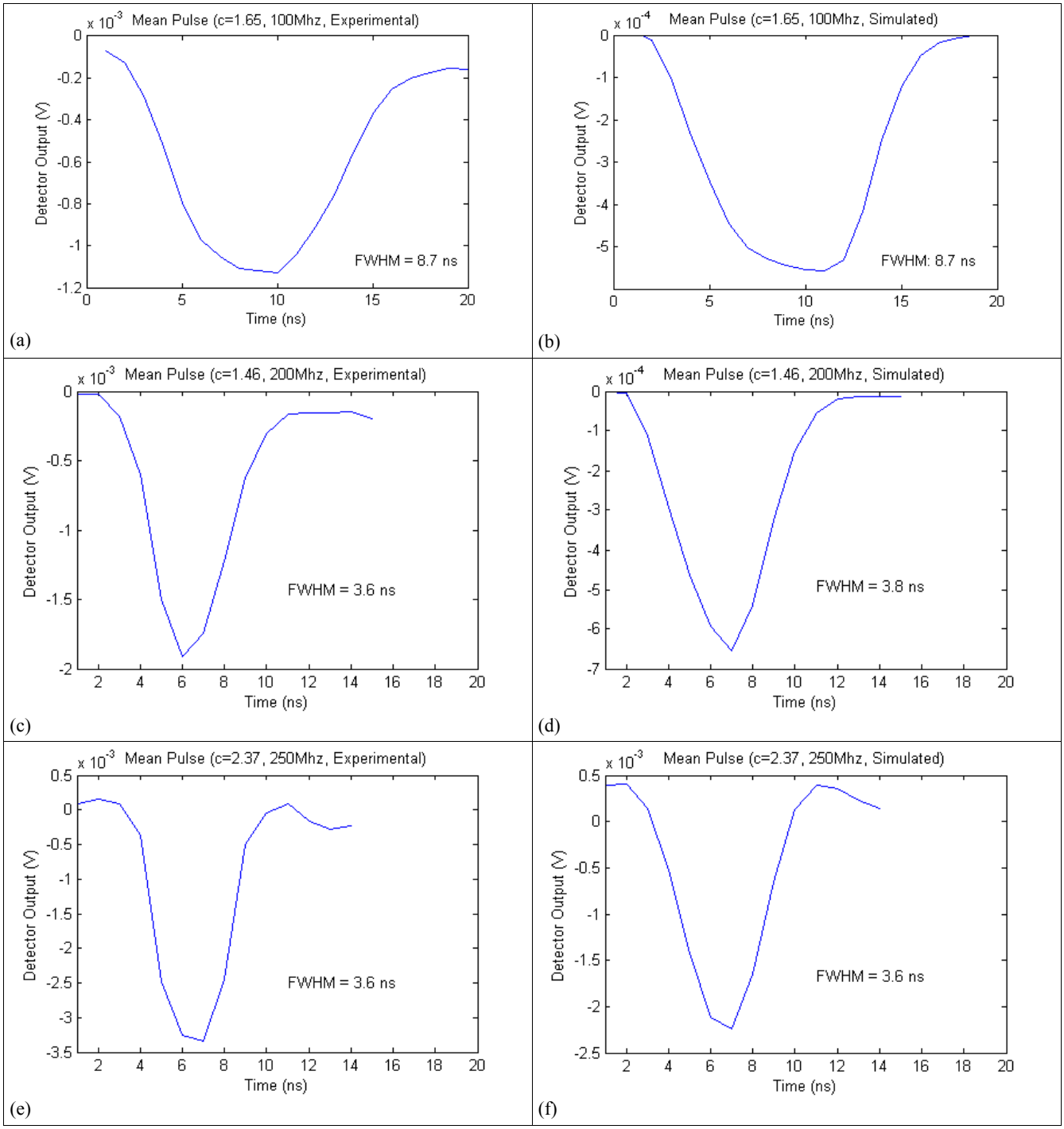

Figure 4: (a)-(f) Successful (correctly demodulated) mean pulses for a selection of turbidities and pulse repetition rates.

5. CONCLUSIONS, DISCUSSION, AND FUTURE WORK

Our physical layer simulator is shown to be an accurate predictor of observed experimental results, with simulated 95% CL BER ceilings within half an order of magnitude in most cases, and all within one order of magnitude. As stated in section 4, more work is needed on modeling the laser source, particularly with respect to the shape of the pulses and the per-pulse variance. Additionally, using symbol error rate (SER) rather than bit error rate (BER) might provide a better performance metric for comparing PPM-16 results, since a single symbol error can result in anywhere from 1 to 4 bit errors.

The demodulator block had no awareness of the pulse stretching effects of the channel and the detector response, but we can see from the mean pulse figures (figures 4(a) - 4(f)), after traveling through the channel, there is a noticeable stretching as a result of multipath scattering in the channel and the detector rise and transit times. At low data rates (longer pulse durations) this may not have a noticeable effect on the signal, but at higher data rates, needs to be taken into account in both simulations and demodulation hardware components in real-world systems.

Now that our physical layer simulator has been verified for on-axis 12.5m distance one-way communication, we will compare it against more test data to ensure the accuracy of the model in more potential real-world scenarios. Of particular interest are the off-axis cases, as this will allow us to more accurately define pointing requirements for Tx/Rx for a given set of IOPs. Note that the one-way version of the channel model was shown in [3] to be an accurate predictor of pulse stretching in off-axis cases in a range of water turbidities, and we expect the one-way model to be similarly accurate in predicting BER ceilings in off-axis cases. Ouyang et. al. [9] demonstrated the feasibility of using the two-way version of our channel model to simulate non line of sight (NLOS) imaging using information-bearing multiple scattered photons, and we plan to use a similar approach in future work to demonstrate conditions under which NLOS communication channels can be achieved. We also plan to use the model to define system requirements for 10^{-4} BER ceiling transmission rates, a set of in-tank and at-sea experiments can then be designed to verify the validity of these requirements. Finally, once all of the validation work is complete, we will integrate the physical layer model with network simulation software to study the higher layer network protocol and the system design parameters for a working real-world system.

ACKNOWLEDGEMENTS

We would like to thank Tom Giddings and Joe Shirron of Metron Inc., for their work in developing the PMT detector model and the Monte Carlo channel model. We would also like to thank Benjamen Metzer, Walter Britton, Brian Ramos, and Drew Krupinski of Harbor Branch Oceanographic Institute for their help in setting up the in-tank experiments. We would also like to thank the Office of Naval Research (ONR) who provided the funding that allowed this research to take place.

REFERENCES

[1] Al-Shamma'a, A., Shaw, A., and Saman, S., "Propagation of Electromagnetic Waves at MHz Frequencies Through Seawater", IEEE TRANSACTIONS ON ANTENNAS AND PROPAGATION, VOL. 52, NO. 11, pp. 2843 – 2849 (2004)

[2] Sozer, E., Stojanovic, M., and Proakis, J., "Underwater Acoustic Networks", IEEE JOURNAL OF OCEANIC ENGINEERING, VOL. 25, NO. 1, pp. 72 – 83 (2000)

[3] Dalgleish, F. R., Caimi, F. M., Vuorenkoski, A. K., Britton, W. B., Ramos, B., "Efficient laser pulse dispersion codes for turbid undersea imaging and communications applications", Proc. SPIE Vol. 7678 Ocean Sensing and Monitoring II, 2010

[4] Larmo, A., Lindstrom, M., Meyer, M., Pelletier, G., Torsner, J., Wiemann, H., "The LTE Link-Layer Design", IEEE Communications Magazine, pp. 52-59 Apr. 2009

[5] Dalgleish, Fraser; Vuorenkoski, Anni; Ouyang, Bing; Caimi, Frank; Shirron, Joseph; Giddings,Thomas; Mazel, Charles, "Experimental and analytical channel impulse Response investigation for distributed laser serial imaging and non line of sight communications sensors in turbid coastal conditions", In Proc. Ocean Optics XXI, Glasgow, UK. October 2012.

[6] Vuorenkoski, A. K., Dalgleish, F. R., Metzger, B., Giddings, T. E. and Shirron, J. J. "Multi-path effects on optical communications links," Proc. ONR/NASA Ocean Optics XX. Sept 27th-Oct 1st 2010. Anchorage, AK.
[7] Jaruwatanadilok, S., "Underwater Wireless Optical Communication Channel Modeling and Performance Evaluation using Vector Radiative Transfer Theory," Selected Areas in Communications, IEEE Journal on , vol.26, no.9, pp.1620,1627, December 2008
[8] Rashkin, D.; Cardei, I.; Cardei, M.; Dalgleish, F.; Giddings, T., "Detector noise model verification for undersea free space optical data links," Oceans, 2012 , vol., no., pp.1,7, 14-19 Oct. 2012
[9] Ouyang, B. Dalgleish, F. R. Vuorenkoski, A.K., Britton, W.B., Ramos B. and Metzger, B., "Visualization for Multi-static Underwater LLS System using Image Based Rendering", IEEE Journal of Oceanic Engineering. 2012. (accepted)